

Bulletin of the Seismological Society of America

Vol. 67

February 1977

No. 1

SURFACE-WAVE CONSTRAINTS ON THE AUGUST 1, 1975, OROVILLE EARTHQUAKE

BY ROBERT S. HART, RHETT BUTLER, HIROO KANAMORI

ABSTRACT

Observations of Love and Rayleigh waves on WWSSN and Canadian Network seismograms have been used to place constraints upon the source parameters of the August 1, 1975, Oroville earthquake. The 20-sec surface-wave magnitude is 5.6. The surface-wave radiation pattern is consistent with the fault geometry determined by the body-wave study of Langston and Butler (1976). The seismic moment of this event was determined to be 1.9×10^{25} dyne-cm by both time-domain and long-period ($T \geq 50$ sec) spectral amplitude determinations. This moment value is significantly greater than that determined by short-period studies. This difference, together with the low seismic efficiency of this earthquake, indicates that the character of the source is intrinsically different at long periods from those aspects which dominate the shorter-period spectrum.

INTRODUCTION

The August 1, 1975 earthquake at Oroville, California [$M_L = 5.9$ (average of PAS and BKS); $m_b = 5.9$ (USGS); $M_s = 5.6$ (average of 25 WWSSN and Canadian Network stations)] has been the object of intense study by many seismologists (Morrison *et al.*, 1975; Ryall and Van Wormer, 1975; Langston and Butler, 1976). This interest is primarily motivated by the proximity of the epicenter to the Oroville Reservoir. We have examined the long-period surface-wave radiation from this event, as recorded at WWSSN and Canadian Network stations in order to place further constraints upon the source mechanism. Events of this rather small magnitude ($M_s = 5.6$) do not ordinarily generate substantial long-period ($T \geq 30$ sec) surface waves. The Oroville surface waves, however, have quite large amplitudes at these periods. This has allowed us to not only confirm the source geometry determined first by Langston and Butler (1976), but also to compute the long-period seismic moment and stress drop for this event. In doing so, we have determined that for long-period energy, the earthquake source is characterized by substantially different parameters than those determined by Langston and Butler (1976) using body-wave data.

DATA AND ANALYSIS

Vertical, long-period seismograms from 25 WWSSN and Canadian Network stations were available to us for this study. The azimuthal coverage obtained with these data is shown in Figure 1. Additionally, the horizontal component seismograms for seven of the WWSSN stations were also obtained. The appropriate great-circle Love-

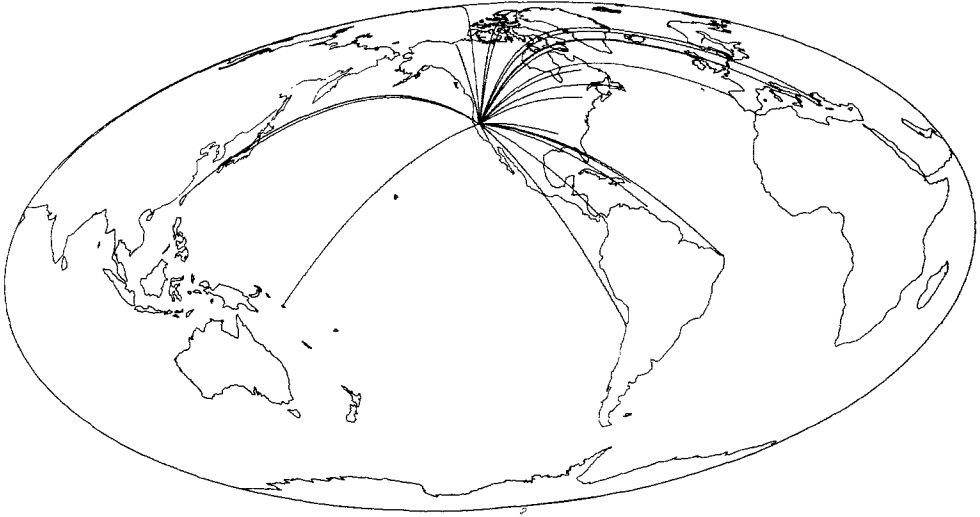


FIG. 1. Great-circle Rayleigh-wave paths used in this study.

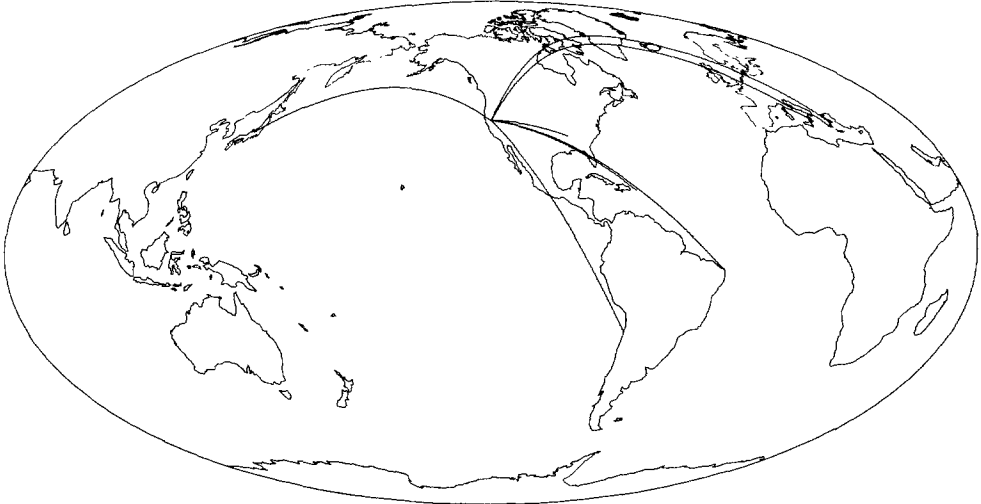


FIG. 2. Great-circle Love-wave paths used in this study.

wave paths for these stations are shown in Figure 2. The Rayleigh and Love waves recorded on all these seismograms were digitized at 1.0 sec intervals. The digitized records were analyzed in both the time and frequency domains in order to extract the source parameters.

Our method of determining the long-period source characteristics of this event is essentially the same as that described previously by Kanamori (1970) and Kanamori and Stewart (1976). The Rayleigh-wave recordings were equalized to a standard distance of 90° and a standard magnification ($\times 1500$). Further the cosine filter

$$W(f) = \begin{cases} \frac{1}{1 - 4 \left(\frac{f}{f_0}\right)^2} \frac{\sin 2\pi(f/f_0)}{2\pi(f/f_0)}, & 0 \leq f \leq f_0 \\ 0, & f > f_0 \end{cases}$$

(where f = frequency and f_0 = cutoff frequency) was applied to remove short-period contributions to the observations. (This filter was applied first with $f_0 = 1/25 \text{ sec}^{-1}$ and then with $f_0 = 1/40 \text{ sec}^{-1}$). The equalized Rayleigh-wave amplitudes thus obtained are plotted in Figure 3 in the standard polar radiation pattern diagram. Because of the lack of observations to the south of the epicenter, we have not attempted to directly connect those points to the west of the epicenter to those to the southeast. The patterns are consistent with the fault geometry determined by the body-wave study of Langston and Butler (1976) (strike = 180° , dip = 65° , slip = -70°) and with the configuration of the aftershock zone (Bufe *et al.*, 1976 and Ryall and Van Wormer, 1975). The theoretical radiation pattern, for the Langston and Butler fault geometry, is computed by using the structure KHC2 (Butler and Kanamori, 1976) and is plotted with the observations in Figure 3. The best fit to the data occurs when a seismic moment of 1.9×10^{25} dyne-cm is assumed. This value is significantly larger, by a factor of more than three, than the 5.7×10^{24} dyne-cm moment determined by Langston and Butler (1976). We considered it necessary, then, to check our moment computations with two other methods before any attempt was made to interpret this discrepancy in terms of the earthquake source.

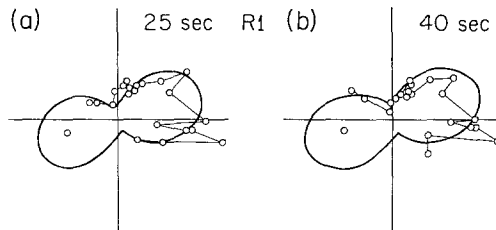


FIG. 3. Observed Rayleigh amplitudes (open circles) equalized to a distance of 90° . (a) High-frequency cutoff at 25 sec. (b) High-frequency cutoff at 40 sec. Solid curves are the theoretical radiation patterns for a seismic moment of 1.9×10^{25} dyne-cm.

Both the Love-wave and the Rayleigh-wave data were Fourier transformed in order to obtain the spectral densities at each observing station. Following the technique of Ben Menahem *et al.* (1970), we computed the seismic moment at each station from the observed spectral densities at periods of 50, 100, and 150 sec. In this computation, the source depth was assumed to be 10 km and a continental structure was used. The average seismic moment thus obtained was 1.85×10^{25} dyne-cm, which agrees well with the equalized amplitude value.

The Love-wave spectral densities yield a seismic moment of 1.6×10^{25} dyne-cm. Since Love waves are more strongly affected by structural heterogeneities than Rayleigh waves, this value is in good agreement with the Rayleigh-wave values. In Table 1 we give the actual moment values in periods of 50 and 100 sec, as determined by the spectral densities, for the loop stations.

As a further check, synthetic Rayleigh waves were computed for each loop station using model KHC2 (Butler and Kanamori, 1976). This structure has a continental crust appropriate to southern California overlying an oceanic mantle. The synthetics were band-pass filtered with a long-period cutoff at 150 sec and with a short-period cutoff at 40 sec.

These band-passed synthetics were compared with similarly band-passed observed Rayleigh waves at these stations. Several of the synthetic Rayleigh waves from each loop are plotted with the corresponding observations in Figure 4. The synthetic wave forms are normalized to the observed amplitudes by assuming the moment value noted with each wave-form pair in this figure. Since model KHC2 has an oceanic-type phase-velocity curve at long periods ($T \geq 40$ sec), the agreement is very good

TABLE 1
 SEISMIC MOMENT VALUES, FROM LOOP STATIONS, AS
 DETERMINED BY THE OBSERVED SPECTRAL
 DENSITIES AT PERIODS OF 50, 100, AND
 150 SECONDS

Station	Period (sec)	Seismic Moment (10^{25} dyne-cm)
MAT	150	1.76
	100	1.83
	50	2.51
SHK	150	3.81
	100	1.56
	50	1.57
HNR	150	1.42
	100	0.70
	50	1.12
TRN	150	2.47
	100	2.07
	50	2.72
SHA	150	
	100	3.33
	50	2.77
STJ	150	1.20
	100	0.74
	50	2.10
SJG	150	3.00
	100	2.04
	50	2.33
PTO	150	1.89
	100	1.04
	50	1.71
MNT	150	1.87
	100	0.93
	50	2.03
BHP	150	2.44
	100	2.30
	50	1.87
NAT	150	2.51
	100	1.31
	50	1.31

for the entire wave train for such stations as MAT and HNR; for stations such as STJ or SHA the agreement is less good beyond the first two or three cycles. However, it is these first two or three cycles that are important for the moment computation.

The moment discrepancy cannot be explained by errors in Q in our computation as Langston and Butler (1976) suggest. The value of Q_R used in the present study is approximately 150 over the period range from 30 to 100 sec. Tsai and Aki (1969) found that Q_R ranges from 120 to 250 in this period range. At a distance of 60° and at 1-min period, a representative distance and period in this study, this uncertainty in Q affects the amplitude by about ± 20 per cent. Thus the error in the moment resulting from the errors in Q is about ± 20 per cent.

With the long-period seismic moment of the Oroville earthquake confirmed at

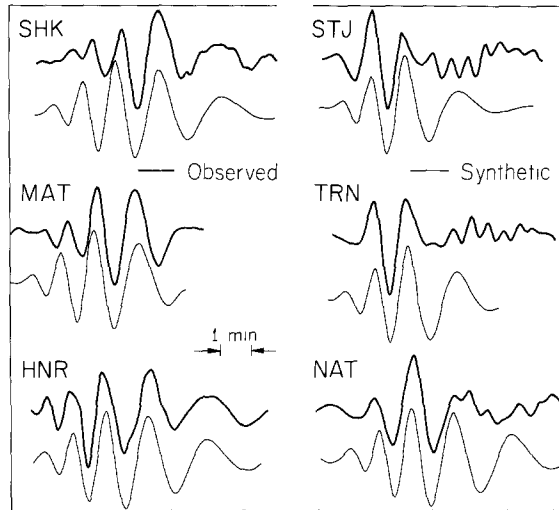


FIGURE 4. Observed and synthetic Rayleigh waves, band-passed at 150 sec and 40 sec, for several loop stations.

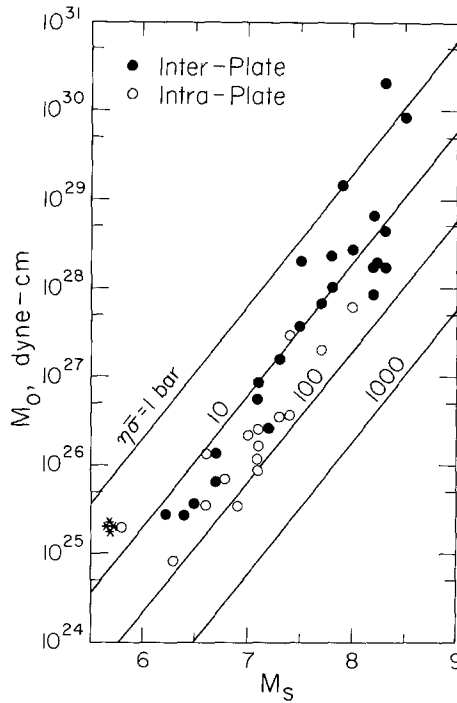


FIG. 5. Relation between M_s (20-sec surface-wave magnitude) and seismic moment. The straight lines are for constant apparent stress. The Oroville earthquake is the star symbol at lower left. (Adapted from Kanamori and Anderson, 1975).

1.9×10^{25} dyne-cm, it is important to consider the resultant implications for the source function of this event. Figure 5, adapted from Kanamori and Anderson (1975), is a plot of the log of the seismic moment versus M_s . From such a diagram, we can obtain the apparent stress of the earthquake source. The Oroville earthquake is plotted as the star symbol in the lower left. Its position indicates an apparent stress of only about 5 bars, very low for an intraplate earthquake.

In Figure 6, also adapted from Kanamori and Anderson (1975), we have plotted the log of the source dimension versus the log of seismic moment from which the stress drop may be determined. The Oroville earthquake again appears as a star symbol in the *lower left*. The stress drop is about 50 bars, roughly the lower bound of values typical of other intraplate events.

Kanamori and Anderson (1975) have shown that, in general, the apparent stress of an earthquake is roughly equal to one-half the observed stress drop. For the Oroville earthquake, however, this ratio is only about one-tenth. This implies a very low seismic efficiency. In light of the large long-period moment, this low efficiency in turn implies that the excitation of seismic energy was "abnormally" biased toward long periods. Thus the discrepancy between the short-period and long-period moment determinations must involve an intrinsic difference in the earthquake source at longer periods.

If the rupture process of this event is bilateral, the time function proposed by Langston and Butler (1976) would suggest that most body-wave energy was radiated

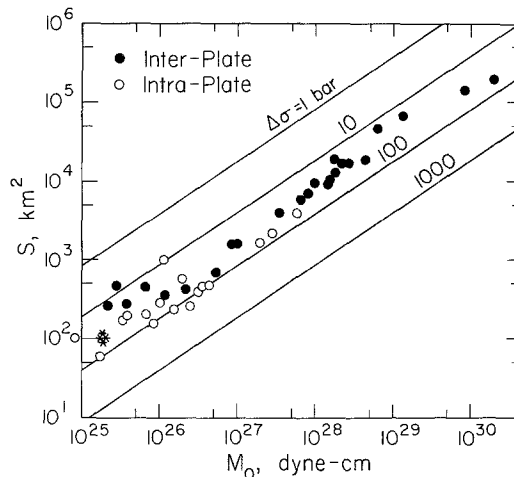


FIG. 6. Relation between fault area and seismic moment. The straight lines are for constant stress drop. The Oroville earthquake is the star symbol at *lower left*. (Adapted from Kanamori and Anderson, 1975.)

from the aftershock area defined by Bufe *et al.* (1975). Then two possibilities may be suggested to explain this discrepancy: (1) The long-period source and the short-period source have approximately the same spatial extent as defined by the aftershock area, but the deformation at the source had long-period components which enhanced the excitation of surface waves. (2) The long-period source involved a larger focal region than the aftershock area; the deformation outside the aftershock area was slow and did not excite short-period body waves.

The far-field body-wave time function is the derivative of the actual displacement time function at the source and, thus, a slow deformation may not be apparent in a body-wave analysis. Such slow deformation could well be pre-seismic, post-seismic, or co-seismic with respect to the conventional *P*-wave onset time of the Oroville earthquake. The present data are not sufficient to distinguish among these possibilities.

Recently, three deep aftershocks of the Oroville earthquake were recorded and located by investigators from the USGS (Hill, personal communication). Two of these events occurred at a depth of 40 km, the third at 20 km. If the fault plane of the main Oroville earthquake is extended to these depths, all three aftershocks lie directly on that plane. This raises the intriguing possibility that the high level of long

period from the Oroville event stems from a slow deformation over a larger focal region extending to much greater depth than the faster, conventional rupture area. If this is the case, the second possibility suggested above may be favored.

CONCLUSION

A detailed analysis of the long-period surface waves from the Oroville earthquake has confirmed the source geometry determined by Langston and Butler (1976). However, both time-domain and frequency-domain computations have yielded a seismic moment of 1.9×10^{25} dyne-cm for this event, approximately three times larger than the moment determined by body-wave data. This larger moment implies a total static displacement of about 50 cm, assuming a fault dimension of 100 km². If a larger fault dimension is involved as suggested above, a smaller displacement would suffice to explain the surface-wave moment. The discrepancy between the short-period-moment value and that determined with long-period data is likely to reflect an intrinsic difference between the source time history affecting different regions of the spectrum.

Preliminary examination of several earthquakes indicates that the phenomena of larger long-period slip may be fairly common. This would be an important development in our overall understanding of earthquake source mechanics.

ACKNOWLEDGMENTS

We would like to thank all the WWSSN stations who were kind enough to send us seismograms for this event. Rhett Butler and Robert S. Hart were supported, respectively, by a Fannie and John Hertz Foundation Fellowship and a National Science Foundation Graduate Fellowship.

This research was supported by NSF Contract EAR 76-14262 and by Advanced Research Projects Agency of the Department of Defense and was monitored by the Air Force Office of Scientific Research under Contract F44620-72-C-0078.

REFERENCES

- Ben-Menahem, A., M. Rosenman, and D. G. Harkrider (1970). Fast evaluation of source parameters from isolated surface-wave signals, *Bull. Seism. Soc. Am.* **60**, 1337.
- Bufe, C. G., F. W. Lester, K. M. Lahr, L. C. Seekins, T. C. Hanks (1976). Oroville earthquakes: normal faulting in the Sierra Nevada foothills, (submitted for publication).
- Butler, R. and H. Kanamori (1976). Long-period ground motion in Los Angeles from a great earthquake on the San Andreas Fault, to be submitted to *Bull. Seism. Soc. Am.*
- Kanamori, H. (1970). Synthesis of long-period surface waves and its application to earthquake source studies—Kurile Island earthquake of October 13, 1963, *J. Geophys. Res.* **75**, 5011.
- Kanamori, H. and D. L. Anderson (1975). Theoretical basis of some empirical relations in seismology, *Bull. Seism. Soc. Am.* **65**, 1073.
- Kanamori, H. and G. S. Stewart (1976). Mode of the strain release along the Gibbs Fracture Zone, Mid-Atlantic Ridge, *Phys. Earth Planet. Interiors* (in press).
- Langston, C. A. and R. Butler (1976). Focal mechanism of the August 1, 1975, Oroville earthquake, *Bull. Seism. Soc. Am.* **66**, 1111–1120.
- Morrison, P., B. Stump, and R. Uhrhammer (1975). The Oroville earthquake sequence and its characteristics, *Trans. Am. Geophys. Union* **56**, 1023.
- Ryall, A. and J. D. Van Wormer (1975). Field study of the August, 1975, Oroville earthquake sequence, *Trans. Am. Geophys. Union* **56**, 1023.
- Tsai, Y. B. and K. Aki (1969). Simultaneous determination of the seismic moment and attenuation of seismic surface waves, *Bull. Seism. Soc. Am.* **59**, 275.

SEISMOLOGICAL LABORATORY
CALIFORNIA INSTITUTE OF TECHNOLOGY
PASADENA, CALIFORNIA 91125
CONTRIBUTION No. 2792

Manuscript received August 19, 1976